Electronic Supplementary Information (ESI) for:

Deep-ultraviolet sulfamate halides with halogen-centered secondary building units for enhanced optical anisotropy

Xuefei Wang, Qingwen Zhu, Yunseung Kuk, Hongheng Chen, Qi Wu,* Qun Jing* and Kang Min Ok*

Table of contents

Table S1. Crystallographic data of $MX(NH_3SO_3)$ (M = Rb, Cs; X = Cl, Br)

	$RbCl(NH_3SO_3)$	**$CsCl(NH_3SO_3)$**	**$RbBr(NH_3SO_3)$**	**$CsBr(NH_3SO_3)$**
Formula weight	218.01	265.45	262.47	309.90
Temp/K	300.0	299.0	299.0	300.0
Crystal system	monoclinic	monoclinic	orthorhombic	orthorhombic
Space group	$P2_1/m$	$P2_1/m$	$Pnma$	$Pnma$
a/Å	4.7178(5)	7.100(2)	13.292(3)	13.9270(9)
b/Å	6.1824(6)	5.5448(17)	5.7921(9)	5.7869(4)
c/Å	9.8402(10)	7.915(3)	7.6673(18)	7.9082(5)
α/°	90	90	90	90
β/°	91.718(3)	102.466(10)	90	90
γ/°	90	90	90	90
V/Å^3	286.88(5)	304.25(17)	590.3(2)	637.35(7)
Z	2	2	4	4
ρ_{calc} g/cm^3	2.524	2.898	2.953	3.230
μ/mm^{-1}	9.362	6.777	15.417	12.320
F(000)	208.0	244.0	488.0	559.1
Crystal size/mm^3	0.259 × 0.143 × 0.108	0.252 × 0.111 × 0.093	0.140 × 0.115 × 0.096	0.189 × 0.124 × 0.102
2 theta range/°	7.786 to 60.93	5.27 to 60.946	6.13 to 60.964	5.86 to 60.98
Index ranges	-6 ≤ h ≤ 6 -8 ≤ k ≤ 8 -14 ≤ l ≤ 14	-10 ≤ h ≤ 10 -7 ≤ k ≤ 7 -11 ≤ l ≤ 11	-18 ≤ h ≤ 18 -7 ≤ k ≤ 4 -10 ≤ l ≤ 10	-19 ≤ h ≤ 16 -8 ≤ k ≤ 8 -11 ≤ l ≤ 11
Reflns collected	5991	7769	5974	10301
Independent reflns	936 (R_{int} = 0.0382)	1010 (R_{int} = 0.0374)	934 (R_{int} = 0.0538)	1049 (R_{int} = 0.0781)
Data/restraints/param	936/2/47	1010/2/45	934/2/48	1049/2/47
Goof on F^2	1.106	1.253	1.053	1.228
R_1[a]/wR_2[b] [I≥2σ (I)]	0.0201/0.0401	0.0198/0.0384	0.0323/0.0768	0.0491/0.0847
R_1[a]/wR_2[b] [all data]	0.0250/0.0410	0.0234/0.0520	0.0543/0.0823	0.0589/0.0875
Largest diff peak/hole / e Å^{-3}	0.44/-0.50	0.63/-0.73	0.77/-0.78	1.33/-1.90

[a]$R_1 = \Sigma||F_o| - |F_o||/\Sigma|F_o|$. [b]$wR_2 = [\Sigma w(F_o^2 - F_c^2)^2/\Sigma wF_o^4]^{1/2}$

Table S2. Fractional atomic coordinates (×10^4), equivalent isotropic displacement parameters (Å^2×10^3) and bond valence sum (BVS) for the non-H atoms in $MX(NH_3SO_3)$ (M = Rb, Cs; X = Cl, Br). U_{eq} is defined as 1/3 of the trace of the orthogonalized U_{ij} tensor.

Atom	*x*	*y*	*z*	*U*(eq)	BVS
			$RbCl(NH_3SO_3)$		
Rb1	3030.4(5)	2500	8283.0(3)	26.2(1)	0.99
Cl1	7879.7(14)	2500	5742.7(6)	26.50(15)	0.24
S1	8797.5(12)	7500	8155.7(6)	18.04(13)	5.89
O1	7792(3)	5541(2)	8756.6(13)	27.6(3)	1.96
O2	11760(4)	7500	7850.5(19)	30.1(4)	1.81
N1	7173(5)	7500	6523(2)	21.6(4)	0.90
			$CsCl(NH_3SO_3)$		
Cs1	6170.5(4)	12500	8266.3(4)	24.94(9)	1.09
Cl1	1333.4(17)	2500	9124.5(16)	28.0(2)	0.40
S1	2645.6(16)	7500	6173.5(14)	20.1(2)	5.88
O1	4134(5)	7500	7719(4)	26.6(7)	2.09
O2	2478(4)	5311(5)	5184(3)	31.7(5)	1.80
N1	547(6)	7500	7037(5)	24.3(8)	0.88
			$RbBr(NH_3SO_3)$		
Rb1	4236.7(5)	2500	1122.2(8)	30.5(2)	0.79
Br1	1978.9(5)	2500	3992.3(8)	26.1(2)	0.43
S1	3617.0(11)	7500	4357.0(18)	19.8(3)	5.79
O1	2867(3)	7500	3009(6)	27.5(10)	1.66
O2	3692(2)	5409(5)	5369(4)	28.5(7)	1.64
N1	4750(4)	7500	3125(7)	22.2(10)	1.22
			$CsBr(NH_3SO_3)$		
Cs1	1965.5(4)	2500	4013.3(6)	22.59(18)	1.08
Br1	4241.8(7)	2500	1121.9(10)	26.6(2)	0.37
S1	3696.4(14)	7500	4377(2)	17.7(4)	5.91
O1	3790(3)	5407(7)	5344(5)	27.0(9)	1.85
O2	2936(4)	7500	3139(7)	27.9(13)	1.94
N1	4729(5)	7500	3090(8)	19.8(13)	0.97

Table S3. Selected bond lengths (Å) and angles (˚) for $RbCl(NH_3SO_3)$.

Rb1-Cl1	3.4388(7)	O1[6]-Rb1-O1[3]	162.18(5)
Rb1-Cl1[3]	3.4336(7)	O1[6]-Rb1-O1[4]	74.16(4)
Rb1-O1[4]	3.1891(14)	O1[5]-Rb1-O1[4]	61.38(4)
Rb1-O1[3]	3.1513(14)	O1[6]-Rb1-O1[5]	101.12(4)
Rb1-O1[5]	3.1513(14)	O1-Rb1-O1[2]	74.16(4)
Rb1-O1[6]	2.9556(13)	O1[2]-Rb1-O1[4]	44.63(5)
Rb1-O1[2]	3.1891(14)	O1[3]-Rb1-O1[4]	88.52(2)
Rb1-O1	2.9556(13)	O1[5]-Rb1-O1[3]	73.27(5)
Rb1-O2[3]	3.1750(5)	O1[6]-Rb1-O1	79.02(5)
Rb1-O2[1]	3.1750(5)	O1[5]-Rb1-O2[1]	45.02(4)
S1-O1	1.4345(13)	O1[3]-Rb1-O2[3]	45.02(4)
S1-O1[7]	1.4345(13)	O1-Rb1-O2[1]	141.27(4)
S1-O2	1.4383(19)	O1[6]-Rb1-O2[3]	141.27(4)
S1-N1	1.759(2)	O1[3]-Rb1-O2[1]	117.07(4)
Cl1[3]-Rb1-Cl1	86.705(17)	O1-Rb1-O2[3]	62.69(4)
O1[5]-Rb1-Cl1	130.49(2)	O1[5]-Rb1-O2[3]	117.07(4)
O1-Rb1-Cl1	66.15(3)	O1[6]-Rb1-O2[1]	62.69(4)
O1[4]-Rb1-Cl1[3]	124.21(3)	O2[1]-Rb1-Cl1[3]	77.04(3)
O1[6]-Rb1-Cl1[3]	129.25(3)	O2[3]-Rb1-Cl1[3]	77.04(3)
O1[4]-Rb1-Cl1	139.98(3)	O2[3]-Rb1-Cl1	91.70(4)
O1[3]-Rb1-Cl1[3]	64.31(2)	O2[1]-Rb1-Cl1	91.70(4)
O1-Rb1-Cl1[3]	129.25(3)	O2[1]-Rb1-O1[4]	74.05(4)
O1[2]-Rb1-Cl1[3]	124.21(3)	O2[3]-Rb1-O1[2]	74.05(4)
O1[2]-Rb1-Cl1	139.98(3)	O2[3]-Rb1-O1[4]	117.68(4)
O1[6]-Rb1-Cl1	66.15(3)	O2[1]-Rb1-O1[2]	117.68(4)
O1[5]-Rb1-Cl1[3]	64.31(2)	O2[3]-Rb1-O2[1]	153.61(6)
O1[3]-Rb1-Cl1	130.49(2)	O1[8]-S1-O1	115.15(12)
O1-Rb1-O1[5]	162.18(5)	O1[8]-S1-O2	114.94(7)
O1[6]-Rb1-O1[2]	102.13(3)	O1-S1-O2	114.94(7)
O1[3]-Rb1-O1[2]	61.38(4)	O1-S1-N1	103.65(7)
O1-Rb1-O1[4]	102.13(3)	O1[8]-S1-N1	103.65(7)
O1-Rb1-O1[3]	101.12(4)	O2-S1-N1	102.05(11)
O1[5]-Rb1-O1[2]	88.52(2)		

[1]-1+*x*, -1+*y*, +*z*; [2]1-*x*, 1-*y*, 2-*z*; [3]-1+*x*, +*y*, +*z*; [4]1-*x*, -1/2+*y*, 2-*z*; [5]-1+*x*,1/2-y,+Z; [6]+*x*, 1/2-*y*, +*z*; [7]+*x*, 3/2-*y*, +*z*; [8]+*x*, 3/2-*y*, +*z*

Table S4. Selected bond lengths (Å) and angles (˚) for $CsCl(NH_3SO_3)$.

Cs1-O2[1]	3.314(3)	O2[6]-Cs1-O2[5]	84.04(5)
Cs1-Cl1[2]	3.6759(11)	O2[1]-Cs1-O2[7]	84.04(5)
Cs1-Cl1[3]	3.5808(17)	O2[1]-Cs1-O2[5]	64.73(7)
Cs1-Cl1[4]	3.6759(11)	O2[7]-Cs1-O2[7]	64.73(7)
Cs1-Cl1[5]	3.6418(16)	O2[6]-Cs1-O2[1]	42.96(9)
Cs1-O2[5]	3.534(3)	O1[4]-Cs1-Cl1[4]	64.78(4)
Cs1-O2[6]	3.314(3)	O1[4]-Cs1-Cl1[2]	64.78(4)
Cs1-O2[7]	3.534(3)	O1[5]-Cs1-Cl1[2]	154.54(7)
Cs1-O1	3.1135(17)	O1[4]-Cs1-Cl1[3]	95.54(6)
Cs1-O1[5]	3.1135(17)	O1[4]-Cs1-Cl1[5]	63.29(6)
Cs1-O1[4]	3.232(4)	O1[5]-Cs1-Cl1[5]	66.28(6)
S1-O2[7]	1.435(2)	O1-Cs1-Cl13	116.87(6)
S1-O2	1.435(2)	O1[5]-Cs1-Cl1[3]	116.87(6)
S1-O1	1.433(3)	O1[5]-Cs1-Cl1[4]	63.88(6)
S1-N1	1.768(4)	O1-Cs1-Cl1[4]	154.54(7)
Cl1[5]-Cs1-Cl1[4]	104.77(2)	O1-Cs1-Cl1[2]	63.88(6)
Cl1[4]-Cs1-Cl1[2]	104.77(2)	O1-Cs1-Cl1[5]	66.28(6)
Cl1[3]-Cs1-Cl1[2]	62.86(2)	O1[5]-Cs1-O2[6]	114.81(8)
Cl1[4]-Cs1-Cl1[2]	97.91(4)	O1[5]-Cs1-O2[7]	92.50(7)
Cl1[3]-Cs1-Cl1[5]	158.83(4)	O1-Cs1-O2[7]	42.12(7)
Cl1[3]-Cs1-Cl1[4]	62.86(2)	O1[5]-Cs1-O2[5]	42.12(7)
O2[5]-Cs1-Cl1[4]	104.54(5)	O1-Cs1-O2[1]	114.81(8)
O2[7]-Cs1-Cl1[2]	104.54(5)	O1[5]-Cs1-O2[1]	76.55(8)
O2[6]-Cs1-Cl1[5]	127.31(5)	O1-Cs1-O2[6]	76.55(8)
O2[6]-Cs1-Cl1[3]	71.93(5)	O1[4]-Cs1-O2[7]	118.80(7)
O2[5]-Cs1-Cl1[2]	156.38(4)	O1[4]-Cs1-O2[5]	118.80(7)
O2[7]-Cs1-Cl1[5]	62.61(5)	O1[4]-Cs1-O2[1]	154.57(5)
O2[7]-Cs1-Cl1[3]	135.01(5)	O1-Cs1-O2[5]	92.50(7)
O2[1]-Cs1-Cl1[5]	127.31(5)	O1[4]-Cs1-O2[6]	154.57(5)
O2[5]-Cs1-Cl1[5]	62.61(5)	O1-Cs1-O1[5]	125.86(11)
O2[7]-Cs1-Cl1[4]	156.38(4)	O1[5]-Cs1-O1[4]	90.53(7)
O2[6]-Cs1-Cl1[4]	123.30(5)	O1-Cs1-O1[4]	90.53(7)
O2[1]-Cs1-Cl1[4]	89.81(5)	O2-S1-O2[7]	115.5(2)
O2[6]-Cs1-Cl1[2]	89.81(5)	O2[7]-S1-N1	103.50(13)
O2[1]-Cs1-Cl1[3]	71.93(5)	O2-S1-N1	103.50(13)
O2[5]-Cs1-Cl1[3]	135.01(5)	O1-S1-O2	115.12(12)
O2[1]-Cs1-Cl1[2]	123.30(5)	O1-S1-O2[7]	115.12(13)
O2[7]-Cs1-O2[5]	52.34(8)	O1-S1-N1	101.4(2)

[1]1-*x*, 2-*y*, 1-*z*; [2]1-*x*, 1-*y*, 2-*z*; [3]1+*x*, 1+*y*, +*z*; [4]1-*x*, 2-*y*, 2-*z*; [5]+*x*, 1+*y*, +*z*; [6]1-*x*, 1/2+*y*, 1-*z*; [7]+*x*, 3/2-*y*, +*z*; [8]+*x*, -1+*y*, +*z*; [9]-1+*x*, -1+*y*, +*z*

Table S5. Selected bond lengths (Å) and angles (˚) for $RbBr(NH_3SO_3)$.

Br1-Rb1[1]	3.6460(13)	N1-Rb1-Br1[7]	78.90(10)
Br1-Rb1[2]	3.6965(7)	N1-Rb1-Br1[8]	67.29(8)
Br1-Rb1[3]	3.6965(7)	N1[11]-Rb1-Br1[7]	78.89(10)
Br1-Rb1	3.7213(11)	N1[10]-Rb1-Br1[7]	66.15(9)
Rb1-N1[5]	3.348(3)	N1[11]-Rb1-Br1	83.86(9)
Rb1-N1	3.348(3)	N1-Rb1-Br1	83.86(9)
Rb1-N1[4]	3.524(5)	N1[11]-Rb1-Br1[9]	67.29(8)
S1-O1	1.436(4)	N1[11]-Rb1-Br1[8]	165.77(10)
S1-O2	1.442(3)	N1[10]-Rb1-Br1[9]	76.05(6)
S1-O2[6]	1.442(3)	N1[10]-Rb1-Br1	148.73(9)
S1-N1	1.778(6)	N1-Rb1-N1[11]	119.76(16)
Br1[7]-Rb1-Br1[8]	115.235(16)	N1[11]-Rb1-N1[10]	110.24(9)
Br1[7]-Rb1-Br1[9]	115.235(16)	N1-Rb1-N1[10]	110.24(9)
Br1[8]-Rb1-Br1	84.765(17)	O1-S1-O2[12]	115.82(15)
Br1[7]-Rb1-Br1	145.13(2)	O1-S1-O2	115.82(15)
Br1[8]-Rb1-Br1[9]	103.15(3)	O1-S1-N1	101.9(3)
Br1[9]-Rb1-Br1	84.765(17)	O2-S1-O2[12]	114.3(3)
N1-Rb1-Br1[9]	165.77(10)	O2-S1-N1	103.13(16)
N1[10]-Rb1-Br1[8]	76.05(6)	O2[12]-S1-N1	103.13(16)

[1]-1/2+*x*, +*y*, 1/2-*z*; [2]1/2-*x*, 1-*y*, 1/2+*z*; [3]1/2-*x*, 1-*y*, 1/2+*z*; [4]1-*x*, 1-*y*, -*z*; [5]+*x*, -1+*y*, +*z*; [6]+*x*, 3/2-*y*, +*z*; [7]1/2+*x*, +*y*, 1/2-*z*; [8]1/2-*x*, 1-*y*, -1/2+*z*; [9]1/2-*x*, -*y*, -1/2+*z*; [10]1-*x*, 1-*y*, -*z*; [11]+*x*, -1+*y*, +*z*; [12]+*x*, 3/2-*y*, +*z*

Table S6. Selected bond lengths (Å) and angles (˚) for $CsBr(NH_3SO_3)$.

Cs1-Br1[1]	3.7390(7)	O1-Cs1-O1[13]	136.59(11)
Cs1-Br1[2]	3.7390(7)	O1-Cs1-O1[11]	110.20(8)
Cs1-S1[3]	3.7809(18)	O1[12]-Cs1-O2	101.83(12)
Cs1-S1[4]	3.7769(13)	O1[12]-Cs1-O2[10]	44.03(12)
Cs1-S1	3.7770(13)	O1-Cs1-O2	44.03(12)
Cs1-O1[5]	3.316(4)	O1[12]-Cs1-O2[8]	68.95(11)
Cs1-O1	3.224(4)	O1-Cs1-O2[10]	101.83(12)
Cs1-O1[6]	3.224(4)	O1-Cs1-O2[8]	68.95(11)
Cs1-O1[3]	3.316(4)	O2-Cs1-Br1[8]	66.11(9)
Cs1-O2[2]	3.266(6)	O2[8]-Cs1-Br1[8]	64.74(5)
Cs1-O2	3.268(3)	O2[10]-Cs1-Br1[9]	66.11(9)
Cs1-O2[4]	3.268(3)	O2-Cs1-Br1[9]	164.93(10)
S1-O1	1.439(4)	O2[8]-Cs1-Br1[9]	64.74(5)
S1-O1[7]	1.439(4)	O2-Cs1-O1[11]	67.84(13)
S1-O2	1.442(6)	O2[10]-Cs1-O1[13]	67.84(13)
S1-N1	1.761(7)	O2[10]-Cs1-O1[11]	105.65(12)
Br1[8]-Cs1-Br1[9]	101.40(2)	O2[8]-Cs1-O1[11]	152.58(10)
O1[12]-Cs1-Br1[9]	78.76(8)	O2-Cs1-O1[13]	105.65(12)
O1-Cs1-Br1[8]	78.76(8)	O2[8]-Cs1-O1[13]	152.58(10)
O1[11]-Cs1-Br1[8]	87.99(7)	O2[10]-Cs1-O2	124.63(18)
O1[13]-Cs1-Br1[8]	122.02(8)	O2[8]-Cs1-O2[11]	101.18(10)
O1[12]-Cs1-Br1[8]	127.78(7)	O2[8]-Cs1-O2	101.18(10)
O1[13]-Cs1-Br1[9]	87.99(7)	O1[14]-S1-O1	114.7(4)
O1-Cs1-Br1[9]	127.78(7)	O1-S1-O2	115.3(2)
O1[11]-Cs1-Br1[9]	122.02(8)	O1[14]-S1-O2	115.3(2)
O1[13]-Cs1-O1[11]	42.85(14)	O1[14]-S1-N1	103.5(2)
O1[12]-Cs1-O1[13]	110.20(8)	O1-S1-N1	103.5(2)
O1-Cs1-O1[12]	62.90(14)	O2-S1-N1	102.0(3)
O1[12]-Cs1-O1[11]	136.59(11)		

[1]1/2-*x*, -*y*, 1/2+*z*; [2]1/2-*x*, 1-*y*, 1/2+*z*; [3]1/2-*x*, 1-*y*, -1/2+*z*; [4]+*x*, -1+*y*, +*z*; [5]1/2-*x*, -1/2+*y*, -1/2+*z*; [6]+*x*, 1/2-*y*, +*z*; [7]+*x*, 3/2-*y*, +*z*; [8]1/2-*x*, 1-*y*, 1/2+*z*; [9]1/2-*x*, -*y*, 1/2+*z*; [10]+*x*, -1+*y*, +*z*; [11]1/2-*x*, 1-*y*, -1/2+*z*; [12]+*x*, 1/2-*y*, +*z*; [13]1/2-*x*, -1/2+*y*, -1/2+*z*; [14]+*x*, 3/2-*y*, +*z*

Table S7. Hydrogen bonds for $RbCl(NH_3SO_3)$.

D-H…A	d_{D-H} (Å)	d_{H-A} (Å)	d_{D-A} (Å)
N1-H1A-Cl1[1]	0.848(15)	2.420(16)	3.2049(7)
N1-H1B-Cl1[2]	0.842(18)	2.72(3)	3.214(2)
N1-H1B-O2[3]	0.842(18)	2.15(2)	2.903(3)

[1]+*x*, 1+*y*, +*z*; [2]1-*x*, 1-*y*, 1-*z*; [3]-1+*x*, +*y*, +*z*

Table S8. Hydrogen bonds for $CsCl(NH_3SO_3)$.

D-H…A	d_{D-H} (Å)	d_{H-A} (Å)	d_{D-A} (Å)
N1-H1A-Cl1[1]	0.826(18)	2.42(2)	3.214(2)
N1-H1B-O2[2]	0.871(19)	2.234(16)	2.916(4)
N1-H1B-O2[3]	0.871(19)	2.234(16)	2.916(4)

[1]+*x*, 1+*y*, +*z*; [2]-*x*, 1-*y*, 1-*z*; [3]-*x*, 1/2+*y*, 1-*z*

Table S9. Hydrogen bonds for $RbBr(NH_3SO_3)$.

D-H…A	d_{D-H} (Å)	d_{H-A} (Å)	d_{D-A} (Å)
N1-H1A-O2[1]	0.84(2)	2.289(18)	2.908(5)
N1-H1B-Br1[2]	0.870(18)	3.57(4)	3.914(6)

[1]1-*x*, 1-*y*, 1-*z*; [2]1/2-*x*, 1-*y*, -1/2+*z*

Table S10. Hydrogen bonds for $CsBr(NH_3SO_3)$.

D-H…A	d_{D-H} (Å)	d_{H-A} (Å)	d_{D-A} (Å)
N1-H1A-Br1[1]	0.853(19)	2.55(3)	3.355(3)
N1-H1B-O1[2]	0.84(2)	2.299(18)	2.936(7)
N1-H1B-O1[3]	0.84(2)	2.299(18)	2.936(7)

[1]+*x*, 1+*y*, +*z*; [2]1-*x*, 1-*y*, 1-*z*; [3]1-*x*, 1/2+*y*, 1-*z*

Table S11. Weight and atomic ratios for $MX(NH_3SO_3)$ (M = Rb, Cs; X = Cl, Br) obtained from SEM-EDX.

	$RbCl(NH_3SO_3)$		$CsCl(NH_3SO_3)$		$RbBr(NH_3SO_3$		$CsBr(NH_3SO_3)$	
Element	**Wt %**	**Atomic %**	**Wt %**	**Atomic %**	**Wt %**	**Atomic %**	**Wt %**	**Atomic %**
Rb	38.24	12.79	/	/	28.81	11.47	/	/
Cs	/	/	39.30	8.43	/	/	37.41	9.87
Cl	15.23	12.28	10.93	8.79	/	/	/	/
Br	/	/	/	/	30.92	13.16	22.56	9.90
O	25.79	46.07	29.17	52.02	20.84	44.32	22.46	49.24
S	11.73	10.46	9.76	8.69	11.80	12.52	9.24	10.11
N	9.01	18.40	10.84	22.07	7.63	18.53	8.33	20.87
Total	100		100		100		100	

Table S12. Calculated and experimental residual weight for $MX(NH_3SO_3)$ (M = Rb, Cs; X = Cl, Br) at 800 °C in TGA.

Compound	**Cal. (%)**	**Exp. (%)**
$RbCl(NH_3SO_3)$	61.24	68.41
$CsCl(NH_3SO_3)$	68.30	73.01
$RbBr(NH_3SO_3)$	50.86	58.12
$CsBr(NH_3SO_3)$	58.41	61.97

Table S13. Assigned vibration peaks for $MX(NH_3SO_3)$ (M = Rb, Cs; X = Cl, Br).

		$RbCl(NH_3SO_3)$	**$CsCl(NH_3SO_3)$**	**$RbBr(NH_3SO_3)$**	**$CsBr(NH_3SO_3)$**
Functional group	**Vibration type**	**Wavenumber (cm^{-1})**			
NH_3	stretching	3166	3161	3202	3207
NH_3	Wagging	2436	2432		
NH_3	bending	1425	1424	1410	1414
SO_3	Antisymmetric and symmetric stretching	1265	1273	1260	1249
		1060	1063	1067	1061
		978	987	990	1002
		691	704	694	680

Table S14. Comparison of the non-π-conjugated optical materials derivatives in the short-wave UV region.

	Compound	Space group	Cut-off edge (nm)	Birefringence	
1	$RbCl(NH_3SO_3)$	$P2_1/m$	185	0.069 @ 546 nm[a]	This work
2	$CsCl(NH_3SO_3)$	$P2_1/m$	185	0.073 @ 546 nm[a]	This work
3	$RbBr(NH_3SO_3)$	*Pnma*	193	0.072 @ 546 nm[a]	This work
4	$CsBr(NH_3SO_3)$	*Pnma*	195	0.075 @ 546 nm[a]	This work
		Phosphates			
5	$NaBaAl(PO_4)_2$	$P2_1/c$	<190	0.005 @ 589 nm[a]	[1]
6	$Na_2Ca_{17}Al_2(PO_4)_{14}$	$R3c$	179	0.012 @ 1064 nm[b]	[2]
7	Mg_2PO_4Cl	$Pna2_1$	<190	0.046 @ 1064 nm[b]	[3]
8	$K_2SrP_4O_{12}$	$I\bar{4}$	<200	0.016 @ 1064 nm[b]	[4]
9	$LiRb_2PO_4$	$Cmc2_1$	<170	0.009 @ 1064 nm[b]	[5]
10	$LiCs_2PO_4$	$Cmc2_1$	174	0.010 @ 1064 nm[b]	[6]
11	$KMg(H_2O)PO_4$	$Pmn2_1$	<200	0.017 @ 1064 nm[b]	[7]
12	KH_2PO_4	$I\bar{4}2d$	180	0.035 @ 1064 nm[a]	[8]
13	$NaBa_2Al(P_2O_7)_2$	$P\bar{1}$	<190	0.007 @ 589 nm[a]	[1]
14	$K_4Mg_4(P_2O_7)_3$	*Pc*	170	0.0108 @ 1064 nm[a]	[9]
15	$RbNaMgP_2O_7$	$Pna2_1/Cmc2_1$	185	0.035 @1064 nm[b]	[10]
16	β-$Cd(PO_3)_2$	$P2_12_12_1$	<190	0.059 @ 1064 nm[b]	[11]
17	$La(PO_3)_3$	$C222_1$	<190	0.040 @ 1064 nm[b]	[11]
18	$CsLa(PO_3)_4$	$P2_1$	167	0.006 @ 1064 nm[b]	[12]
19	$RbBa_2(PO_3)_5$	*Pc*	163	0.009 @ 1064 nm[b]	[13]
20	$KLa(PO_3)_4$	$P2_1$	163	0.0084 @ 1064 nm[b]	[14]
21	$Ba_3P_3O_{10}Cl$	$Pca2_1$	180	0.028 @ 1064 nm[b]	[15]
22	$Ba_3P_3O_{10}Br$	$P2_12_12_1$	<200	0.023 @ 1064 nm[b]	[15]
23	$LiHgPO_4$	$P4_2/m$	<300	0.0068 @ 1064 nm[b]	[16]
24	$K_2TeP_2O_8$	$P2_12_12_1$	270	0.05 @ 1064 nm[b]	[18]
25	$CsMgPO_4{\cdot}6H_2O$	$P6_3/mmc$	258	0.006 @ 1064 nm[b]	[18]
26	$RbMgPO_4{\cdot}6H_2O$	$Pmn2_1$	288	0.005 @ 1064 nm[b]	[18]
		Sulfates			
27	$Li_8NaRb_3(SO_4)_6{\cdot}2H_2O$	*C*2	<190	0.021 @ 1064 nm[a]	[19]
28	$NH_4NaLi_2(SO_4)_2$	*C*2	<186	0.008 @ 1064 nm[b]	[20]
29	$La(NH_4)(SO_4)_2$	$Pmn2_1$	<190	0.03 @1064 nm[b]	[21]
30	$LiKSO_4$	$P6_3$	160	0.03 @ 1064 nm[b]	[22]
31	$LiN_2H_5SO_4$	$Pna2_1$	<190	0.0126 @1064 nm[b]	[23]
32	$K_2Zn_3(SO_4)(HSO_4)_2F_4$	$Cmc2_1$	<200	0.01268 @ 546 nm[a]	[24]
33	$KZnSO_4F$	$Pna2_1$	<190	0.022 @ 550 nm[b]	[25]
34	$KMgSO_4F$	$Pna2_1$	170	0.012 @ 550 nm[b]	[26]
35	KSO_3CF_3	$P2_1$	156	0.017 @ 1064 nm[b]	[27]
36	α-$RbSO_3CF_3$	*Cm*	<200	0.035 @ 1064 nm[b]	[28]

37	β-$RbSO_3CF_3$	$P2_1$	<200	0.034 @ 1064 nm[b]	[28]
38	$CsSO_3CF_3$	$P2_1$	<200	0.027 @ 1064 nm[b]	[29]
39	$KYSO_4F_2$	$P2_1/m$	<190	0.015 @ 546.1 nm[a]	[30]
40	$RbYSO_4F_2$	$P2_1/m$	<190	0.02 @ 546.1 nm[a]	[30]
41	$(NH_4)_2BeS_2O_8$	$I\bar{4}2d$	<200	0.019 @ 546.1 nm[a]	[31]
42	$K_2BeS_2O_8$	$I\bar{4}2d$	<200	0.024 @ 546.1 nm[a]	[31]
43	$Rb_2BeS_2O_8$	$I\bar{4}2d$	<200	0.024 @ 546.1 nm[a]	[31]
44	$Cs_2BeS_2O_8$	$I\bar{4}2d$	<200	0.013 @ 546.1 nm[a]	[31]
45	$Li_2SO_4·H_2O$	$P2_1$	240	0.023 @ 1064 nm[b]	[32]
46	$K_2Bi_2(SO_4)_2Cl_4$	$P2_12_12_1$	278	0.056 @ 1064 nm[b]	[33]
47	$(NH_{4)2}Bi_2(SO_4)_2C_{l4}$	$P2_12_12_1$	273	0.055 @ 1064 nm[b]	[33]
48	$Rb_2Bi_2(SO_4)_2Cl_4$	$P2_12_12_1$	276	0.047 @ 1064 nm[b]	[33]
49	$Rb_3In(SO_4)_3$	$R3c$	215	0.019 @ 1064 nm[b]	[34]
50	$Sb_6O_7(SO_4)_2$	$Ccc2$	286	0.052 @ 1064 nm[b]	[35]
51	$CsY(SO_4)_2·4H_2O$	$P2_1/c$	200	0.045 @ 546 nm[b]	[36]
52	$NaRbY_2(SO_4)_4$	$C2/c$	200	0.045 @ 550 nm[a]	[37]
53	$NaBi(SO_4)_2·H_2O$	$P3_22_1$	280	0.068 @ 546 nm[a]	[38]
54	$ZrF_2(SO_4)$	$Pca2_1$	206	0.052 @ 1064 nm[a]	[39]
55	$(NH_4)_2S_2O_3$	$C2$	238	0.077 @ 546 nm[a]	[40]
		Sulfamates			
56	$Pb(NH_2SO_3)_2·H_2O$	$P2_1/c$	226	0.032 @ 1064 nm[b]	[41]
57	$Pb(NH_2SO_3)_2$	$P2_1/c$	208	0.023 @ 1064 nm[b]	[41]
58	$Ca(NH_2SO_3)_2·4H_2O$	$C2/c$	<200	0.025 @ 1064 nm[b]	[41]
59	$Ca(NH_2SO_3)_2·H_2O$	$P2_12_12_1$	<200	0.033 @ 1064 nm[b]	[41]
60	$Cs_2Mg(NH_2SO_3)_4·4H_2O$	Cm	<180	0.054 @ 546.1 nm[a]	[42]
61	$K_2Ca(NH_2SO_3)_4$	$P\bar{1}$	<200	0.035 @ 523 nm[b]	[42]
62	$Rb_2Ca(NH_2SO_3)_4$	$P\bar{1}$	<200	0.036 @ 523 nm[b]	[42]
63	$Cd(NH_2SO_3)_2·2H_2O$	$P\bar{1}$	212	0.052 @ 1064 nm[b]	[43]
64	$Cd(NH_2SO_3)_2$	$P2_12_12_1$	210	0.037 @ 1064 nm[b]	[43]
65	$Ba(SO_3NH_2)_2$	$Pna2_1$	<190	0.028 @ 546.1 nm[a]	[44]
66	$Sr(SO_3NH_2)_2$	Pc	<190	0.056 @ 589.3 nm[a]	[44]
		Others			
67	NH_3BH_3	$I4mm$	<190	0.056 @ 550 nm[a]	[45]
68	$KN(SO_2F)_2$	$Pbca$	182	0.061 @ 546 nm[b]	[46]
69	$(NH_4)_2PO_3F$	$Pna2_1$	176	0.035 @ 532 nm[b]	[47]
70	$NaNH_4PO_3F·H_2O$	Pn	176	0.053 @ 532 nm[b]	[48]
71	Na_2PO_3F	$P2_12_12_1$	<190	0.036 @ 532 nm[b]	[49]
72	$KHPO_3F$	$P2_1$	<190	0.028 @ 532 nm[b]	[50]
73	$NaPO_3NH_3$	$P6_3$	<190	0.062 @ 546.1 nm[a]	[51]
74	$Ba(SO_3CH_3)_2$	$Cmc2_1$	159	0.04 @ 589.3 nm[a]	[52]
75	$Na_2S_3O_6$	$Fdd2$	212	0.056 @ 546 nm[a]	[53]
76	$K_2S_4O_6$	Cc	298	0.066 @ 1064 nm[b]	[54]

[a]Measured birefringence, [b]calculated birefringence.

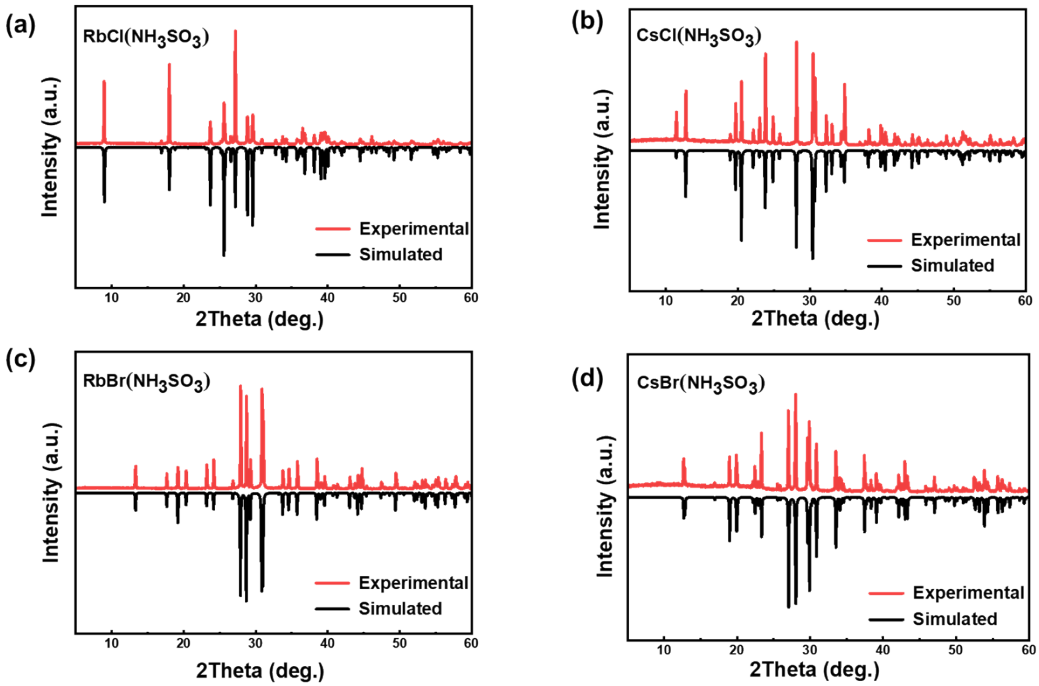

Figure S1. Experimental and simulated PXRD patterns for $MX(NH_3SO_3)$ (M = Rb, Cs; X = Cl, Br).

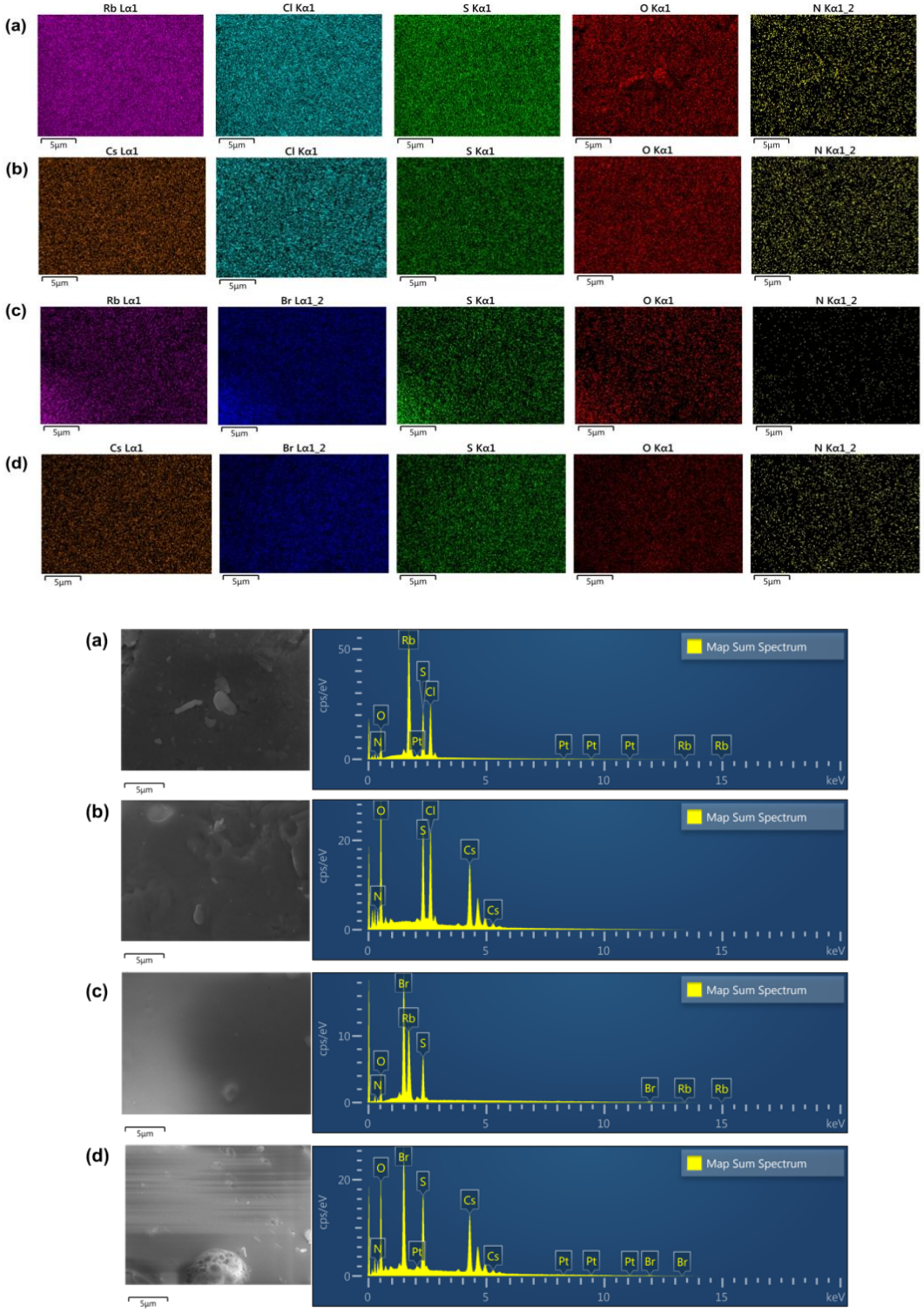

Figure S2. SEM-EDX for $MX(NH_3SO_3)$ (M = Rb, Cs; X = Cl, Br).

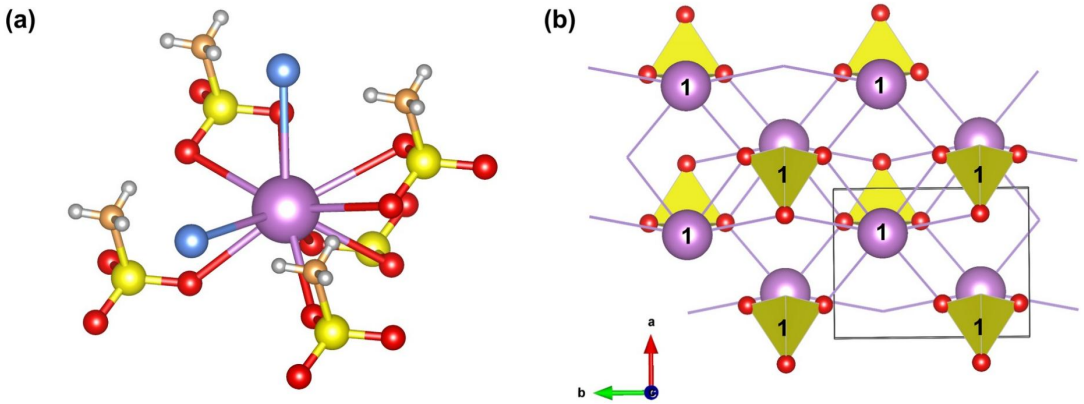

Figure S3. (a) The asymmetric unit and (b) pseudo-doubled layer along the *ab* planes for $RbCl(NH_3SO_3)$.

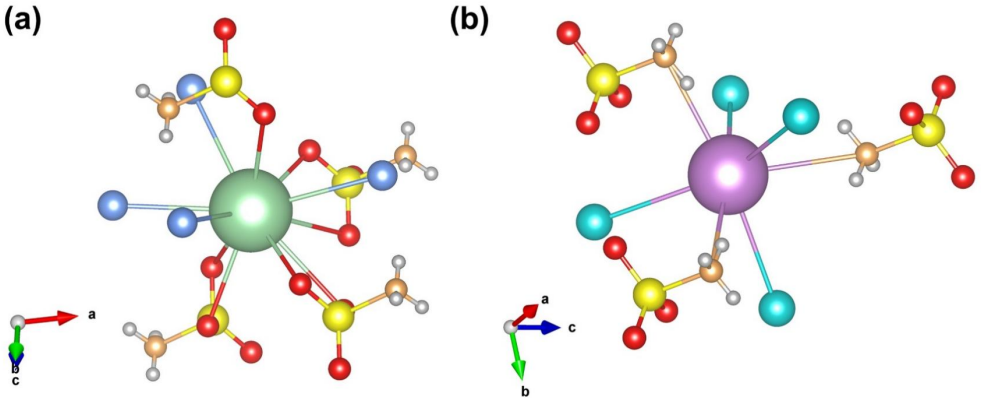

Figure S4. (a) The asymmetric unit for $CsCl(NH_3SO_3)$ and (b) the asymmetric unit for $RbBr(NH_3SO_3)$.

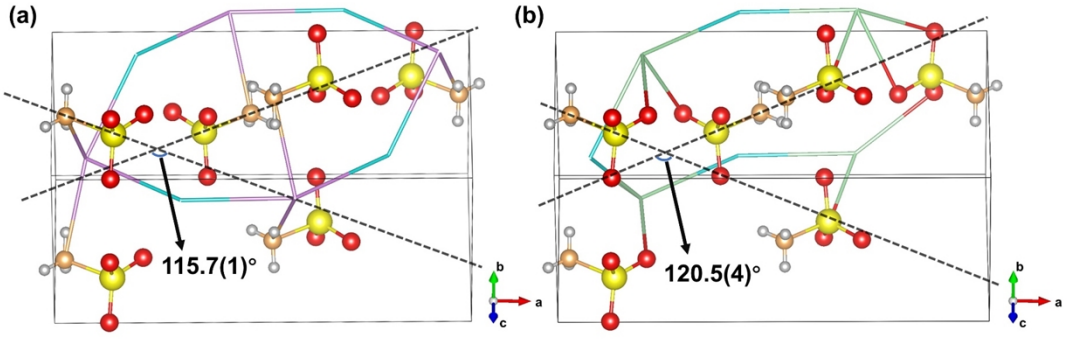

Figure S5. The intersection angle of the NH_3SO_3 tetrahedra in (a) $RbBr(NH_3SO_3)$ and (b) $CsBr(NH_3SO_3)$.

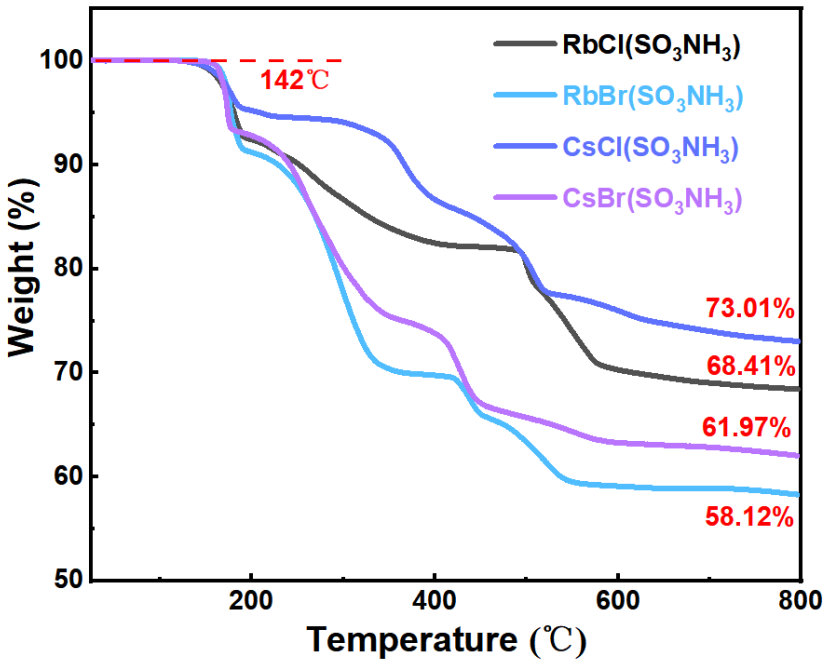

Figure S6. TGA diagrams for $MX(NH_3SO_3)$ (M = Rb, Cs; X = Cl, Br).

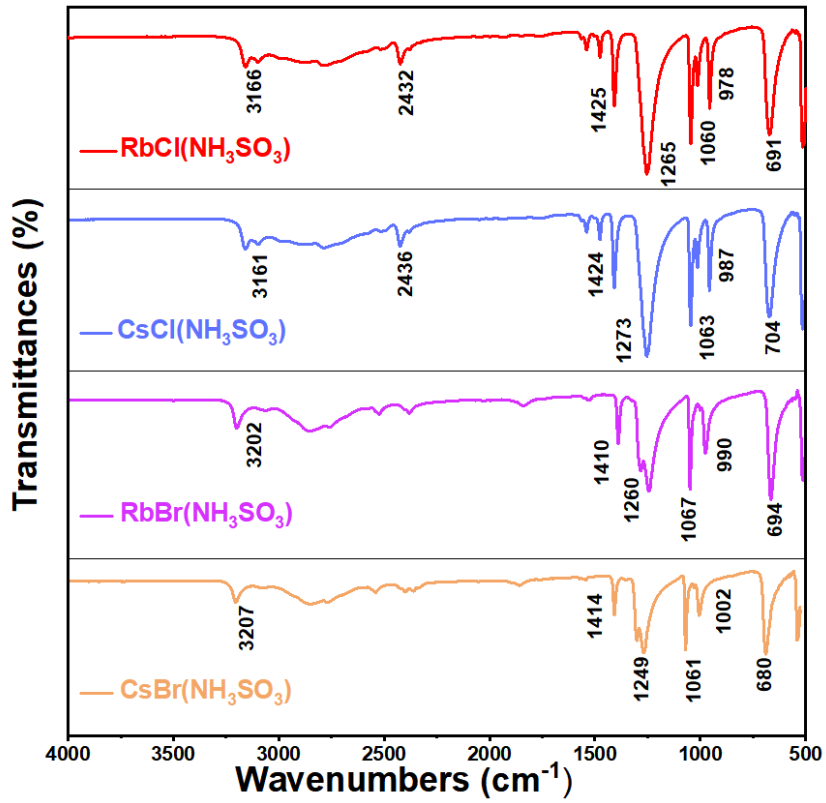

Figure S7. IR spectra for $MX(NH_3SO_3)$ (M = Rb, Cs; X = Cl, Br).

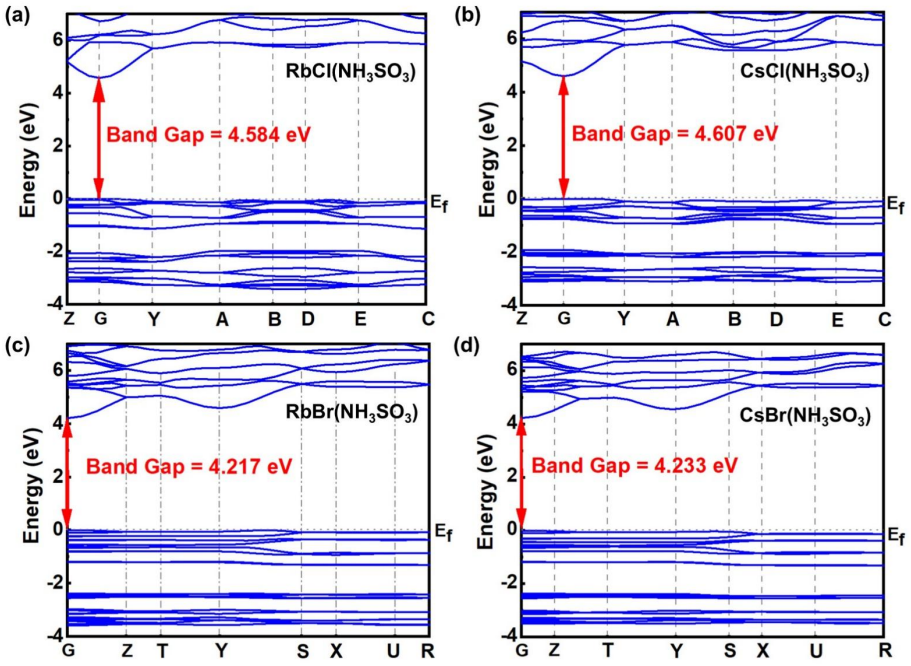

Figure S8. Band structures of compounds for $MX(NH_3SO_3)$ (M = Rb, Cs; X = Cl, Br).

References

1 F. Wang, X.-N. Yao, Y. Guo, L. Yang, Y.-G. Chen and X.-M. Zhang, Insights into Varying Dimension Structures for Deep-UV Optical Crystals $NaBa_2Al(P_2O_7)_2$ and $NaBaAl(PO_4)_2$ Constructed Separately from Unique $[Al(P_2O_7)_2]$ Chains and $[Al(PO_4)_2]$ Layers, *J. Solid. State. Chem.*, 2021, **301**, 8.

2 Y.-G. Chen, X. Yu, Y. Guo, Y. Xue, X. H. Hao, X. Yao and X.-M. Zhang, Ca-cluster-constructed Deep-Ultraviolet Nonlinear-optical Crystal $Na_2Ca_{17}Al_2(PO_4)_{14}$ with Strong NLO Response, *J. Alloy. Compd.*, 2022, **896**, 6.

3 J.-X. Zhang, Q.-G. Yue, S.-H. Zhou, X.-T. Wu, H. Lin and Q.-L. Zhu, Screening Strategy Identifies an Overlooked Deep-Ultraviolet Transparent Nonlinear Optical Crystal, *Angew. Chem. Int. Ed.*, 2024, **63**, 7.

4 Z. Bai, L. Liu, L. Zhang, Y. Huang, F. Yuan and Z. Lin, $K_2SrP_4O_{12}$: a deep-UV Transparent Cyclophosphate as a Nonlinear Optical Crystal, *Chem. Commun.*, 2019, **55**, 8454–8457.

5 L. Li, Y. Wang, B.-H. Lei, S. Han, Z. Yang, H. Li and S. Pan, $LiRb_2PO_4$: a New Deep-ultraviolet Nonlinear Optical Phosphate with a Large SHG Response, *J. Mater. Chem. C*, 2017, **5**, 269–274.

6 X. Cheng, M.-H. Whangbo, G.-C. Guo, M. Hong and S. Deng, Large Second-Harmonic Generation of $LiCs_2PO_4$ is caused by the Metal-Cation-Centered Groups, *Angew. Chem. Int. Ed.*, 2018, **57**, 3933-3937.

7 Z. Bai, C.-L. Hu, L. Liu, L. Zhang, Y. Huang, F. Yuan and Z. Lin, $KMg(H_2O)PO_4$: A Deep-Ultraviolet Transparent Nonlinear Optical Material Derived from $KTiO_PO_4$, *Chem. Mat.*, 2019, **31**, 9540–9545.

8 J. De Yoreo, A. Burnham and P. Whitman, Developing KH_2PO_4 and KD_2PO_4 Crystals for The World's Most Power Laser, *Inter. Mater. Rev.*, 2002, **47**, 113–152.

9 H. Yu, J. Young, H. Wu, W. Zhang, J. M. Rondinelli and P. S. Halasyamani, $M_4Mg_4(P_2O_7)_3$ (M = K, Rb): Structural Engineering of Pyrophosphates for Nonlinear Optical Applications, *Chem. Mat.*, 2017, **29**, 1845–1855.

10 X. Yang, S. Zhao, S. Geng, L. Yang, Q. Huang, X. Kuang, J. Luo and X. Xing, Structural Origin of Thermally Induced Second Harmonic Generation Enhancement in $RbNaMgP_2O_7$, *Chem. Mat.*, 2019, **31**, 9843–9849.

11 J. Lv, Y. Qun, Q. Jing, X. Wang, M.-H. Lee and Z. Chen, Two Metal Phosphate Nonlinear Optical Materials Simultaneously Exhibiting Ultraviolet Transparence and a Large Birefringence, *Chem. Mat.*, 2022, 9.

12 T. Sun, P. Shan, H. Chen, X. Liu, H. Liu, S. Chen, Y. Cao, Y. Kong and J. Xu, Growth and Properties of a Noncentrosymmetric Polyphosphate $CsLa(PO_3)_4$ Crystal with Deep-ultraviolet Transparency, *Crystengcomm*, 2014, **16**, 10497–10504.

13 S. Zhao, P. Gong, S. Luo, L. Bai, Z. Lin, C. Ji, T. Chen, M. Hong and J. Luo, Deep-Ultraviolet Transparent Phosphates $RbBa_2(PO_3)_5$ and $Rb_2Ba_3(P_2O_7)_2$ Show Nonlinear Optical Activity from Condensation of $[PO_4]^{3-}$ Units, *J. Am. Chem. Soc.*, 2014, **136**, 8560–8563.

14 P. Shan, T. Sun, H. Chen, H. Liu, S. Chen, X. Liu, Y. Kong and J. Xu, Crystal Growth and Optical Characteristics of Beryllium-free Polyphosphate, $KLa(PO_3)_4$, a Possible Deep-ultraviolet Nonlinear Optical Crystal, *Sci. Rep.*, 2016, **6**, 25201.

15 P. Yu, L.-M. Wu, L.-J. Zhou and L. Chen, Deep-ultraviolet nonlinear optical crystals: $Ba_3P_3O_{10}X$ (X= Cl, Br), *J. Am. Chem. Soc.*, 2014, **136**, 480–487.

16 B.-L. Wu, C.-L. Hu, F.-F. Mao, R.-L. Tang and J.-G. Mao, Highly Polarizable Hg^{2+} Induced a Strong Second Harmonic Generation Signal and Large Birefringence in $LiHgPO_4$, *J. Am. Chem. Soc.*, 2019, **141**, 10188-10192.

17 M. Wen, C. Hu, Z. Yang, X. Wu and S. Pan, $K_2TeP_2O_8$: a New Telluro-phosphate with a Pentagonal Te-P-O Layer Structure, *Dalton Trans.*, 2018, **47**, 9453–9458.

18 Y. Zhou, L. Cao, C. Lin, M. Luo, T. Yan, N. Ye and W. Cheng, $AMgPO_4 \cdot 6H_2O$ (A= Rb, Cs): Strong SHG Responses Originated from Orderly PO_4 Groups, *J. Mater. Chem. C*, 2016, **4**, 9219–9226.

19 Y. Li, S. Zhao, P. Shan, X. Li, Q. Ding, S. Liu, Z. Wu, S. Wang, L. Li and J. Luo, $Li_8NaRb_3(SO_4)_6 \cdot 2H_2O$ as a New Sulfate Deep-ultraviolet Nonlinear Optical Material, *J. Mater. Chem. C*, 2018, **6**, 12240–12244.

20 Y. Li, F. Liang, S. Zhao, L. Li, Z. Wu, Q. Ding, S. Liu, Z. Lin, M. Hong and J. Luo, Two Non-π-conjugated Deep-UV Nonlinear Optical Sulfates, *J. Am. Chem. Soc.*, 2019, **141**, 3833–3837.

21 C. Wu, X. Jiang, Y. Hu, C. Jiang, T. Wu, Z. Lin, Z. Huang, M. G. Humphrey and C. Zhang, A Lanthanum Ammonium Sulfate Double Salt with a Strong SHG Response and Wide Deep-UV Transparency, *Angew. Chem. Int. Ed.*, 2022, **61**, e202115855.

22 C. Amirthakumar, B. Valarmathi, P. Pandi and R. M. Kumar, Investigation on Inorganic Potassium Lithium Sulfate Single Crystal Grown by SR Method and Its Characterization for Nonlinear Optical Application, *Chin. J. Phys.*, 2020, **67**, 305–313.

23 T. F. T. Fukami and R.-H. C. R.-H. Chen, Crystal Structure and Electrical Conductivity of $LiN_2H_5SO_4$ at High Temperature, *Jpn. J. Appl. Phys.*, 1998, **37**, 925.

24 Y. Zhou, X. Zhang, Z. Xiong, X. Long, Y. Li, Y. Chen, X. Chen, S. Zhao, Z. Lin and J. Luo, Non-π-Conjugated Deep-ultraviolet Nonlinear Optical Crystal $K_2Zn_3(SO_4)(HSO_4)_2F_4$, *J. Phys. Chem. Lett.*, 2021, **12**, 8280–8284.

25 Y. Zhou, X. Liu, Z. Lin, Y. Li, Q. Ding, Y. Liu, Y. Chen, S. Zhao, M. Hong and J. Luo, Pushing $KTiOPO_4$-like Nonlinear Optical Sulfates into the Deep-Ultraviolet Spectral Region, *Inorg. Chem.*, 2021, **60**, 18950–18956.

26 A. Poddar, S. Gedam and S. Dhoble, Development of Orange-red Emitting Phosphors and Studies of Thermoluminescence Characteristics of $KMgSO_4F$ Material, *J. Lumin.*, 2014, **149**, 245–250.

27 S. Ko, Y. Yamada and A. Yamada, A 62 m K-ion Aqueous Electrolyte, *Electrochem. Commun.*, 2020, **116**, 106764.

28 L. Hildebrandt, R. Dinnebier and M. Jansen, Crystal Structure and Ionic Conductivity of Three Polymorphic Phases of Rubidium Trifluoromethyl Sulfonate, $RbSO_3CF_3$, *Inorg. Chem.*, 2006, **45**, 3217–3223.

29 B. Xu, P. Gong, F. Liu, X. Zhang, H. Huo and Z. Lin, $(SO_3CF_3)^-$: A Non-π-Conjugated Motif for Nonlinear Optical Crystals Transparent into the Deep-Ultraviolet Region, *Adv. Opt. Mater.*, 2024, **12**, 2301725.

30 Z. Wu, H. Li, X. Hou, Z. Yang and H. Shi, $AYSO_4F_2$(A= K, Rb):$[YO_4F_4]$ Polyhedra Enhancement of Birefringence in Non-π-Conjugated Sulfate Systems, *Inorg. Chem.*, 2024, **63**, 4783–4789.

31 Y. Sun, C. Lin, H. Tian, Y. Zhou, J. Chen, S. Yang, N. Ye and M. Luo, $A_2BeS_2O_8$ (A = NH_4, K, Rb, Cs) Deep Ultraviolet Nonlinear Optical Crystals, *Chem. Mat.*, 2022, **34**, 3781–3788.

32 P. Becker, S. Ahrweiler, P. Held, H. Schneeberger and L. Bohatý, Thermal expansion, Pyroelectricity and Linear Optical Properties of $Li_2SeO_4 \cdot H_2O$ and $Li_2SO_4 \cdot H_2O$, *Cryst. Res. Technol.*, 2003, **38**, 881–889.

33 K. Chen, Y. Yang, G. Peng, S. Yang, T. Yan, H. Fan, Z. Lin and N. Ye, $A_2Bi_2(SO_4)_2Cl_4$ (A=NH_4, K, Rb): Achieving a Subtle Balance of the Large Second Harmonic Generation Effect and Sufficient Birefringence in Sulfate Nonlinear Optical Materials, *J. Mater. Chem. C*, 2019, **7**, 9900–9907.

34 Q. Xu, X. Jiang, C. Wu, L. Lin, Z. Huang, Z. Lin, M. G. Humphrey and C. Zhang, $Rb_3In(SO_4)_3$: a

Defluorinated Mixed Main-group Metal Sulfate for Ultraviolet Transparent Nonlinear Optical Materials with a Large Optical Band Gap, *J. Mater. Chem. C*, 2021, **9**, 5124–5131.

35 Q. Wei, C. He, K. Wang, X.-F. Duan, X.-T. An, J.-H. Li and G.-M. Wang, $Sb_6O_7(SO_4)_2$: A Promising Ultraviolet Nonlinear Optical Material with an Enhanced Second-Harmonic-Generation Response Activated by SbIII Lone-Pair Stereo Activity, *Chem. Eur. J.*, 2021, **27**, 5880–5884.

36 Y. Shen, L. Huang, Z. Wang, Y. Zhou, X. Xue, H. Lin, R. Yan, S. Zhao and J. Luo, $CsY(SO_4)_2{\cdot}4H_2O$: a Deep-Ultraviolet Birefringent Crystal induced by an Edge-sharing Connection, *Inorg. Chem.*, 2022, **61**, 4468-4475.

37 Y. Zhao, Y. Song, Y. Li, W. Liu, Y. Zhou, W. Huang, J. Luo, S. Zhao and B. Ahmed, Deep-Ultraviolet Bialkali-Rare Earth Metal Anhydrous Sulfate Birefringent Crystal, *Inorg. Chem.*, 2024.

38 S. Cheng, Y. Wu, D. Mei, S. Wen and T. Doert, Synthesis, Crystal Structures, Spectroscopic Characterization, and Thermal Analyses of the New Bismuth Sulfates $NaBi(SO_4)_2{\cdot}H_2O$ and $ABi(SO_4)_2$ (A= K, Rb, Cs), *Z. Anorg. Allg. Chem.*, 2020, **646**, 1688–1695.

39 C. Wu, C. Jiang, G. Wei, X. Jiang, Z. Wang, Z. Lin, Z. Huang, M. G. Humphrey and C. Zhang, Toward Large Second-harmonic Generation and Deep-UV Transparency in Strongly Electropositive Transition Metal Sulfates, *J. Am. Chem. Soc.*, 2023, **145**, 3040–3046.

40 S. Ke, H. Fan, C. Lin, N. Ye and M. Luo, Constructing Ultraviolet Nonlinear Optical Crystals with Large Second Harmonic Generation and Short Absorption Edges by using Polar Tetrahedral S_2O_3 Groups, *Inorg. Chem. Front.*, 2023, **10**, 2811–2817.

41 D. Dou, B. Cai, B. Zhang and Y. Wang, $M(NH_2SO_3)_2{\cdot}xH_2O$ (M= Ca, Pb, x= 0, 1, 4): Effect of Hydrogen Bonding on Structural Transformations and Second Harmonic Generation of Metal Sulfamates, *Inorg. Chem.*, 2022, **61**, 21131–21138.

42 X. Wang, X. Leng, Y. Kuk, J. Lee, Q. Jing and K. M. Ok, Deep-Ultraviolet Transparent Mixed Metal Sulfamates with Enhanced Nonlinear Optical Properties and Birefringence, *Angew. Chem. Int. Ed.*, 2024, **63**, e202315434.

43 X. Wang, J. Lee, Y. Li, Y. Kuk and K. M. Ok, $Cd(NH_2SO_3)_2{\cdot}xH_2O$ (x= 0, 2): New Sulfamates with a Unique Coordination Environment and Reversible Phase Transitions, *Inorg. Chem. Front.*, 2023, **10**, 1411–1420.

44 H. Fan, N. Ye and M. Luo, New Functional Groups Design toward High Performance Ultraviolet Nonlinear Optical Materials, *Acc. Chem. Res.*, 2023, **56**, 3099–3109.

45 Y. Zhou, N. He, Z. Lin, X. Shang, X. Chen, Y. Li, W. Huang, M. Hong, S. Zhao and J. Luo, A Non-π-Conjugated Molecular Crystal with Balanced Second-Harmonic Generation, Bandgap, and Birefringence, *Small*, 2024, **20**, 2305473.

46 K. Matsumoto, T. Oka, T. Nohira and R. Hagiwara, Polymorphism of Alkali Bis (fluorosulfonyl) Amides ($M[N(SO_2F)_2]$, M= Na, K, and Cs), *Inorg. Chem.*, 2013, **52**, 568–576.

47 L. Xiong, J. Chen, J. Lu, C.-Y. Pan and L.-M. Wu, Monofluorophosphates: a New Source of Deep-ultraviolet Nonlinear Optical Materials, *Chem. Mat.*, 2018, **30**, 7823–7830.

48 Q. Ding, X. Zhang, Z. Lin, Z. Xiong, Y. Wang, X. Long, S. Zhao, M. Hong and J. Luo, Designing a Deep-UV Nonlinear Optical Monofluorophosphate, *Sci. China Chem.*, 2022, **65**, 1710–1714.

49 W. Jin, C. Xie, X. Hou, M. Cheng, E. Tikhonov, M. Wu, S. Pan and Z. Yang, From Monofluorophosphates A_2PO_3F to Difluorophosphates APO_2F_2 (A= alkali metal): Design of a Potential Deep-ultraviolet Nonlinear Optical Materials System with a Shortened Phase-matching Wavelength, *Chem. Mat.*, 2023, **35**, 5281–5290.

50 H. A. Prescott, S. I. Troyanov and E. Kemnitz, The Crystal Structures of the Potassium Hydrogen

Monofluorophosphates, $KHPO_3F$ and $K_3[H(PO_3F)_2]$, and the α Modification of $RbHPO_3F$, *Z. Kristallogr. Cryst. Mater.*, 2003, **218**, 604–611.

51 L. Wu, H. Tian, C. Lin, X. Zhao, H. Fan, P. Dong, S. Yang, N. Ye and M. Luo, Optimized Arrangement of Non-π-conjugated PO_3NH_3 Units Leads to Enhanced Ultraviolet Optical Nonlinearity in $NaPO_3NH_3$, *Inorg. Chem. Front.*, 2024, **11**, 1145–1152.

52 H. Tian, C. Lin, X. Zhao, F. Xu, C. Wang, N. Ye and M. Luo, $Ba(SO_3CH_3)_2$: A Deep-Ultraviolet Transparent Crystal with Excellent Optical Nonlinearity Based on a New Polar Non-π-Conjugated NLO Building Unit $SO_3CH_3^-$, *CCS Chem.*, 2023, **5**, 2497–2505.

53 H. Sha, Y. Shang, Z. Wang, R. Su, C. He, X. Yang and X. Long, A Sharp Improvement of Sulfate's Birefringence Induced by the Synergistic Effect of Heteroleptic and Dimeric Strategies, *Small*, 2024, **20**, 2309776.

54 T. Huang, Y. Xiao, J. Gu, Y. Wang, K. Wu and B. Zhang, $K_2S_4O_6$: Improving Birefringence and Nonlinear Optical Properties with the $[O_3S\text{-}S\text{-}S\text{-}SO_3]^{2-}$ Group, *J. Mater. Chem. C*, 2022, **10**, 17190–17195.